JACS
JOURNAL OF THE AMERICAN CHEMICAL SOCIETY
Article
pubs.acs.org/JACS

Ultrafast Observation of a Solvent Dependent Spin State Equilibrium in CpCo(CO)

Justin P. Lomont, Son C. Nguyen, Jacob P. Schlegel, Matthew C. Zoerb, Adam D. Hill, and Charles B. Harris*

Department of Chemistry, University of California, Berkeley, California 94720, United States and Chemical Science Division, Lawrence Berkeley National Laboratory, Berkeley, California 94720, United States

Supporting Information

ABSTRACT: We report the observation of a solvent-dependent spin state equilibrium in the 16-electron photoproduct CpCo(CO). Time-resolved infrared spectroscopy has been used to observe the concurrent formation of two distinct solvated monocarbonyl photoproducts, both of which arise from the same triplet CpCo(CO) precursor. Experiments in different solvent environments, combined with electronic structure theory calculations, allow us to assign the two solvated photoproducts to singlet and triplet CpCo(CO)(solvent) complexes. These results add to our previous picture of triplet reactivity for 16-electron organometallic photoproducts, in which triplets were not believed to interact strongly with solvent molecules. In the case of this photoproduct, it appears that spin crossover does not present a significant barrier to reactivity, and relative thermodynamic stabilities determine the spin state of the CpCo(CO) photoproduct in solution on the picosecond time scale. While the existence of transition metal complexes with two thermally accessible spin states is well-known, this is, to our knowledge, the first observation of a transient photoproduct that exhibits an equilibrium between two stable spin states, and also the first observed case in which a solvent has been able to coordinate as a token ligand to two spin states of the same photoproduct.

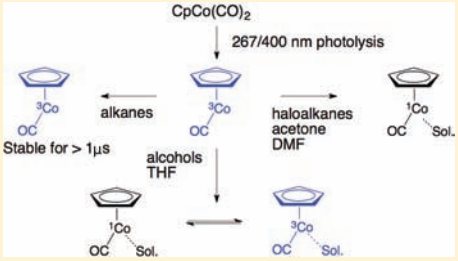

I. INTRODUCTION

Cyclopentadienyl cobalt dicarbonyl is widely used as a catalyst for the cyclotrimerization of alkynes,[1] and its time-resolved photochemistry has been studied by several authors.[2−7] Experimental and theoretical investigations have established that the primary photoproduct, CpCo(CO), exists in a triplet ground state in the gas phase and in alkane solutions, but that reactivity of CpCo(CO) typically occurs via the singlet state.[7−10] Interestingly, theoretical predictions have shown that a ligand-bound minimum can exist for both the singlet and triplet species[9,10] and that the identity of an incoming ligand affects the relative energies of the bound singlet and triplet states. Figure 1 illustrates this unique feature of the triplet potential energy surface of CpCo(CO), relative to other triplet photoproducts. Here we use time-resolved infrared spectroscopy (TRIR) to explore whether cases exist in which a solvent-coordinated triplet state is preferred over that of a singlet or whether it is possible to observe two solvated spin states simultaneously.

Previous solution-phase studies on the reactivity of CpCo(CO) and other triplet organometallic photoproducts have suggested that triplet photoproducts interact very weakly with alkyl groups of solvent molecules and that spin crossover to a singlet state is necessary for the coordination of a solvent molecule to the unsaturated metal center.[5−7,11−20] The rate of spin state interconversion depends heavily on the solvent environment, however, and coordinating solvents can increase the rate of spin crossover for unsaturated triplet species.[10]

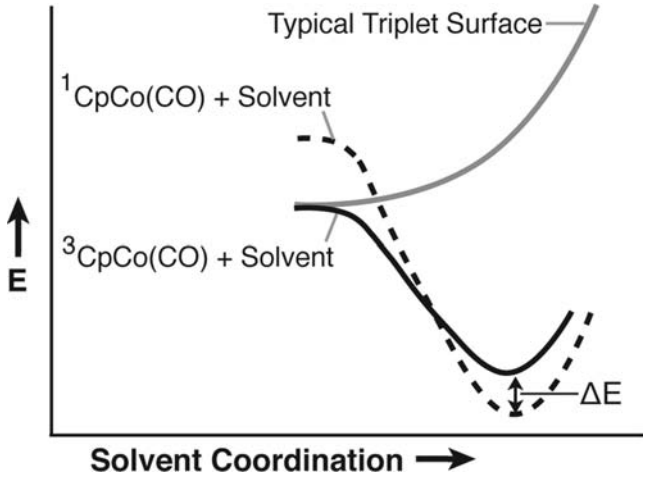

Figure 1. Schematic potential energy surfaces for solvent coordination to CpCo(CO), compared to more typical triplet 16-electron species. Many triplets show a predominantly repulsive potential toward solvent coordination (solid gray line), while the triplet surface for CpCo(CO) shows an attractive potential (solid black line). ΔE designates the energy difference between solvated singlet and triplet states.

The lack of solvent coordination to unsaturated triplet species has been shown to play an important role in their

Received: October 19, 2011
Published: January 12, 2012

 © 2012 American Chemical Society dx.doi.org/10.1021/ja2098468 | J. Am. Chem.Soc. 2012, 134, 3120−3126

reactivity, exemplified by studies on the activation of Si−H bonds in triethylsilane.[15−20] Because they interact so weakly with alkyl groups, triplets diffuse more rapidly through the alkyl chains in neat triethyl silane solutions than their singlet counterparts. Upon encountering a more coordinating Si−H bond, however, triplets readily undergo spin crossover to allow bond activation. This combination of factors allows triplet photoproducts to activate Si−H bonds much more rapidly than those formed in a singlet state, despite the fact that one might expect these reactions to be spin-blocked.

Our observation of a solvent coordinated triplet CpCo(CO) species in this study would be consistent with previous computational studies showing that a ligand-bound minimum can exist on the triplet surface.[9,10] Computational mechanistic studies have also implicated triplet intermediates in alkyne cyclotrimerization reactions catalyzed by this species.[21] To facilitate interpretation of the experimental results, we use density functional theory (DFT) to study each of the solvent-coordinated photoproducts observed in this study. We investigate the choice of various density functionals on the relative spin state energies, and consistent with the earlier careful study by Carreón−Macedo and Harvey,[10] the BP86 and PW91 functionals appear to give reasonably accurate results for the relative spin state energetics of CpCo(CO).

II. METHODS

A. Sample Preparation. $CpCo(CO)_2$ was purchased from Strem Chemicals Inc. All solvents were purchased from Sigma-Aldrich Co. All samples and solvents were used without further purification. Dilute solutions of $CpCo(CO)_2$ were stable in air at ambient temperatures for at least a few hours (verified via FTIR) in all solvents. Samples used to collect TRIR spectra were prepared at a concentration of ca. 5 mM.

B. Ultrafast UV/Visible-Pump-IR Probe Spectroscopy. The experimental setup consists of a Ti:sapphire regenerative amplifier (SpectraPhysics, Spitfire) seeded by a Ti:sapphire oscillator (SpectraPhysics, Tsunami) to produce a 1 kHz train of 100 fs pulses centered at 800 nm with an average pulse power of 1.1 mJ. The output of this commercial system is split, and 30% of the output is used to generate 400 and 267 nm pump pulses (80 and 6 μJ per pulse at sample, respectively) via second and third harmonic generation. The other 70% is used to pump a home-built two-pass BBO-based optical parametric amplifier (OPA),[22] the output of which is mixed in a $AgGaS_2$ crystal to produce mid-IR probe pulses tunable from 3.0 to 6.0 μm with a 200 cm^{-1} spectral width and a ca. 100 fs pulse duration. The 400 and 267 nm pulses pass through a 25 cm silica rod, which stretches the pulses in time to 1 ps and gives a cross correlation of the mid-IR and 400 or 267 nm pulses of 1.1 ps at the sample. The stretched 400 and 267 nm pulses are necessary to achieve high pump powers without generating products resulting from multi-photon excitation. The stretched pulses also reduce artifacts resulting from nonlinear optical effects in the sample cell windows.

The polarization of the pump beam is held at the magic angle (54.7°) with respect to the mid-IR probe beam to eliminate effects from rotational diffusion. A computer controlled translation stage (Newport) allows for variable time delays up to ca. 1.5 ns between pump and probe pulses. The sample is flowed using a mechanical pump through a stainless steel cell (Harrick Scientific) fitted with 2 mm thick CaF_2 windows separated by 150 μm spacers. The pump and probe beams are spatially overlapped at the sample and focused so that the beam diameters are ca. 200 and 100 μm respectively. The sample cell is moved by computer controlled translational stages (Standa) during the course of data collection so that absorptions are not altered by any accumulation of photoproduct on the sample windows. Reference and signal mid-IR beams are sent along a parallel path across the table, before being directed into a computer controlled spectrograph with entrance slits set at 70 μm (Action Research Corporation, SpectraPro-150) and detected by a 2 × 32 element MCT-array IR detector (InfraRed Associates, Inc.) and a high-speed signal acquisition system and data-acquisition software (Infrared Systems Development Corp.) with a resolution of ca. 2.5 cm^{-1}. Collected signals are averaged over 20000 laser shots to correct for shot-to-shot fluctuations. Differences in optical density as small as 5×10^{-5} are observable after 1 s of data collection.

C. Quantum Chemical Modeling. The ground spin state of CpCo(CO) has been investigated previously be several authors.[8−10] In this case, we were particularly interested in the relative spin-state energetics of CpCo(CO) coordinated to different solvent molecules, so we carried out geometry optimizations using three different density functionals (BP86,[23] B3LYP,[23a,24] PW91[25]) in the Gaussian09 package.[26] The aug-cc-pDVZ basis set[27] was used in all calculations, except those involving 1-iodobutane. Since the aug-cc-pDVZ basis is not defined for iodine, the lanl2dz[28,29] basis was used on the iodine atom, while the aug-cc-pDVZ basis was used for all other atoms in these calculations. All geometry optimizations were followed with a frequency analysis for use in interpreting the TRIR results, and also to verify that the calculated geometries were genuine local minima. For the potential energy surface scans shown in Figure 5, the distance between the Co atom of CpCo(CO) and the O atom of methanol was held fixed at various distances as the remaining geometrical parameters were optimized. These calculations were performed for both singlet and triplet CpCo(CO) species to locate an approximate minimum energy crossing point (MECP) for the coordination of methanol to CpCo(CO), as described in section III.D.

To investigate the strength of spin−orbit coupling (SOC) between the singlet and triplet spin states, complete active space multi-configurational self-consistent field (casscf) calculations were carried out in the GAMESS-US package[30] using Ahlrich's pDVZ basis set[31] with one additional d function on each C and O atom, and an additional f function on Co. The BP86 geometry for ^{3}CpCo(CO) was used in these calculations (calculated geometries were similar for each choice of DFT functional). The active space of the casscf calculations consisted of 8 electrons in 10 d-type orbitals, constituting an (8,10) active space. The choice to include unoccupied d-type orbitals containing an extra node was made to account for the double−shell effect, which has been shown to be important in transition metal complexes.[32] Calculations were performed as follows: restricted or restricted open shell Hartree−Fock calculations were performed for singlet and triplet states, respectively, to generate the initial wave functions. After inspecting the active space orbitals, the casscf wave function was generated for the triplet state. The core orbitals from the triplet casscf wave function are then frozen in the subsequent calculation of the singlet casscf wave function, as this is necessary for the corresponding orbital transformation necessary to calculate the SOC matrix elements.[33] Finally, SOC between singlet and triplet states was calculated using the full Breit-Pauli spin-orbit Hamiltonian.[34] This method of calculating SOC is favorable, as it allows for different molecular orbitals to describe the ground and excited states. The effects of state averaging when generating the casscf wave functions were tested but did not result in a meaningful difference in calculated SOC values, and the reported result is based on wave functions that were not state averaged.

III. RESULTS AND DISCUSSION

The TRIR spectra in the CO stretching region are presented as difference absorbance spectra. Positive absorptions correspond to newly formed species, while negative bands correspond to the depletion of parent molecules. Since the negative parent bands are very similar in each case, the spectra presented focus on the newly formed product peaks.

A. Ultrafast UV-Pump IR-Probe Spectroscopy in Alkanes and Haloalkanes. The photochemistry of $CpCo(CO)_2$ in alkane solutions has been studied by several authors.[3,6,7] In cyclohexane, the carbonyl loss photoproduct, ^{3}CpCo(CO), forms in a triplet ground state with a characteristic IR absorption at 1989 cm^{-1} and is stable as a triplet for >1

dx.doi.org/10.1021/ja2098468 | J. Am. Chem.Soc. 2012, 134, 3120−3126

μs.[2] We wanted to investigate whether spin crossover and solvent coordination would occur on the picosecond time scale in more coordinating solvent environments, so we carried out the same experiment in a series of haloalkanes: 1-chlorobutane, 1-bromobutane, and 1-iodobutane.

In each of these solvents, ^{3}CpCo(CO) was not directly observed, but instead a product peak at ca. 1935 cm^{-1} was present (Figure 2 and Table 2). On the basis of electronic structure calculations of the relative spin state energetics of the CpCo(CO) molecule interacting with each haloalkane (section III.D), we assign this photoproduct to a solvated singlet species. We conclude that spin crossover to a ^{1}CpCo(CO)(sol.) photoproduct takes place within the first several picoseconds of the formation of the CpCo(CO) photoproduct in these halogenated solvents, and no evidence of other solvated photoproducts was observed.

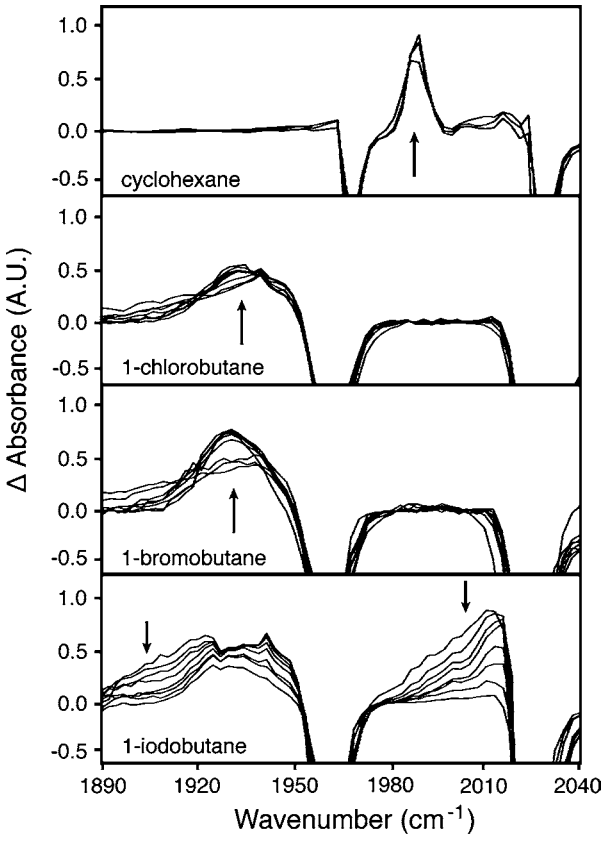

Figure 2. TRIR spectra of $CpCo(CO)_2$ in cyclohexane and haloalkane solvents at 10, 30, and 50 ps (cyclohexane), and 5, 10, 20, 30, 40, 50, 60, and 70 ps (haloalkanes) following 267 nm photolysis (400 nm photolysis was used in the case of 1−iodobutane, which also results in a broad absorption corresponding to an electronically excited state).

For spectra taken in 1-iodobutane solvent, 400 nm excitation was used to avoid a strong UV-absorption band of 1-iodobutane that prevents photolysis of $CpCo(CO)_2$ using 267 nm pump pulses. This results in the formation of CpCo(CO) along with an electronically excited state of $CpCo(CO)_2$ with a lifetime of ca. 50 ps, as can be observed in the spectra in Figure 2.[35] TRIR spectra were also recorded in the other solvents using 400 nm photolysis, and the same photochemistry involving the CpCo(CO) photoproduct was observed in each, indicating that both spectra result in the same CO loss photochemistry and thus can be directly compared. All other spectra are presented using 267 nm excitation.

B. Ultrafast UV-Pump IR-Probe Spectroscopy in Acetone and DMF. We next studied the photolysis of $CpCo(CO)_2$ in acetone and dimethylformamide (DMF), which are expected to be more strongly coordinating than haloalkanes via their sp^2 hybridized oxygen atoms. Figure 3 shows the TRIR spectra of $CpCo(CO)_2$ in acetone and DMF.

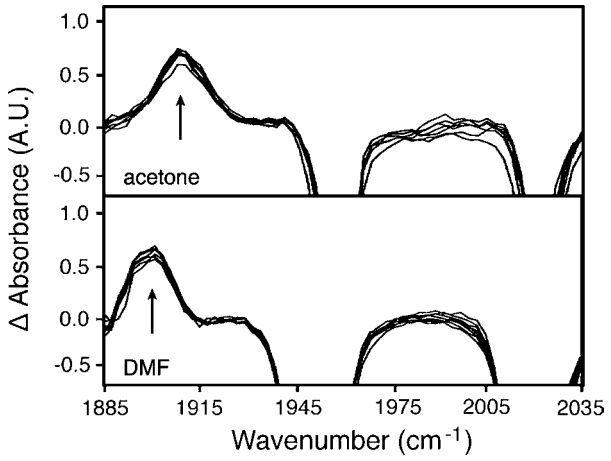

Figure 3. TRIR spectra of $CpCo(CO)_2$ in neat acetone and DMF solvents at 5, 10, 20, 30, 40, 50, 60, and 70 ps following 267 nm photolysis.

In both acetone and DMF, only a single photoproduct is observed. The frequency of this product's absorption is significantly red-shifted compared to the solvated singlet observed in the haloalkane solvents. DFT calculations (section III.D) predict this to be the case for solvated singlet CpCo(CO), and also confirm that the singlet species is the more stable spin state. On this basis, we assign this photoproduct to a ^{1}CpCo(CO)(sol.) species.

C. Ultrafast UV−Pump IR−Probe Spectroscopy in Alcohols and THF. We next wanted to study the photolysis of $CpCo(CO)_2$ in alcohol and THF solvents, as we felt the sp^3 oxygen atoms in these solvents would provide an interesting comparison to the sp^2 hybridized oxygen atoms in acetone and DMF. Shown in Figure 4 are the TRIR spectra of $CpCo(CO)_2$ in methanol, 1-butanol, 1-hexanol, 1-decanol, and THF.

Interestingly, these spectra reveal the presence of two distinct solvated photoproducts at ca. 1916 and 1942 cm^{-1}. In 1-butanol, 1-hexanol, and 1-decanol, unsolvated ^{3}CpCo(CO) can also be initially observed via its IR absorption at ca. 1989 cm^{-1}, and this decays within 50 ps. This is readily explained by the fact that the longer alkyl chains require ^{3}CpCo(CO) to, on average, undergo more diffusion before encountering a −OH site to which it can coordinate. This is consistent with our previous understanding of the interactions of triplet species with alkyl groups.[11] The presence of two peaks at ca. 1916 and 1942 cm^{-1} was surprising, however, and their assignment requires more detailed explanation.

We performed these experiments using both 267 and 400 nm pump pulses, and observed that the ratio of peaks at ca. 1916 and 1942 cm^{-1} was independent of the pump wavelength. Comparison to experiments in acetone and DMF (section III.C) confirms that these peaks arise from two distinct chemical species. This information, combined with the observed kinetics in the longer chain alcohol solvents, indicates

dx.doi.org/10.1021/ja2098468 | J. Am. Chem.Soc. 2012, 134, 3120−3126

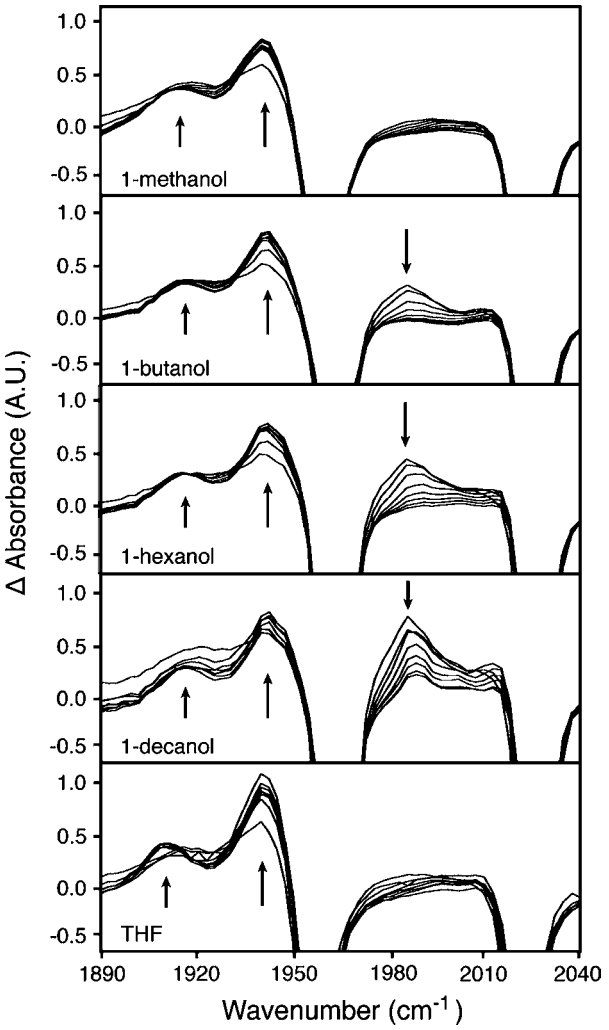

Figure 4. TRIR spectra of $CpCo(CO)_2$ in neat alcohol and THF solvents at 5, 10, 20, 30, 40, 50, 60, and 70 ps following 267 nm photolysis. In 1-butanol, 1-hexanol, and 1-decanol, the initially unsolvated $^3CpCo(CO)$ species can be observed at ca. 1989 cm^{-1}.

that the peaks at 1916 and 1942 cm^{-1} correspond to two distinct photoproducts originating from the same precursor, which in this case is $^3CpCo(CO)$. Though we initially considered that one of these peaks could belong to a ring-slipped species, this is inconsistent with the understanding of why ring-slip takes place. Ring slippage would only decrease the electron count on an already electron deficient 16-electron metal center, which is inconsistent with observations of ring-slip in the literature.[36] To determine whether a weak interaction with a second solvent molecule could be responsible for one of the two observed photoproducts species, we also obtained the TRIR spectra in diluted solutions (10 and 50 mol %) of 1-butanol or THF in cyclohexane. These spectra in diluted alcohol solutions showed essentially the same peak ratios at ca. 1916 and 1942 cm^{-1}, indicating that no weak interaction with a second alcohol or THF molecule, such as hydrogen bonding with the Cp ring, are responsible for the presence of a second species. A solvent hydrogen bond donor is also ruled out by the very similar spectra in both alcohols and THF. Having thus ruled out all other reasonable possibilities, we are able to conclude that the oxygen atom in alcohol and THF solvents is able to coordinate to CpCo(CO) in both singlet and triplet spin states. This conclusion is supported by the results of electronic structure calculations comparing the energetics of each alcohol coordinated to singlet and triplet CpCo(CO) (section III.D). By comparing the observed and calculated frequencies and calculated spin state energy differences for CpCo(CO) in each solvent, we were able to assign the lower frequency peak at ca. 1916 cm^{-1} to $^1CpCo(CO)$(sol.), and the higher frequency peak at ca. 1942 cm^{-1} to $^3CpCo(CO)$(sol.).

We note that both products form at essentially the same rate from the unsolvated $^3CpCo(CO)$ precursor and that they form in the same ratio at which they are present at 1.5 ns within the first ca. 10 ps, or roughly during the vibrational cooling period of the nascent photoproduct. This implies that there is little barrier to spin crossover from the unsolvated $^3CpCo(CO)$ precursor, and we infer it is likely that both solvated spin states are in equilibrium. We will examine this point in more detail in section III.D.

One previous study[6] has investigated the time-resolved IR spectrum of $CpCo(CO)_2$ in dilute alkane solutions containing THF on the microsecond time scale, but these authors did not report the observation of a second peak at ca. 1916 cm^{-1}, which we have assigned to solvated $^1CpCo(CO)$. One possible explanation is that $^1CpCo(CO)$(sol.) is more reactive than $^3CpCo(CO)$(sol.) on longer time scales, and thus it has already reacted prior to the shortest time delay (0.5 μs) reported in that work. This conflicts, however, with the fact that we believe there to be little barrier to equilibration of $^3CpCo(CO)$(sol.) and $^1CpCo(CO)$(sol.). Looking carefully at the spectra from that work, an alternative explanation is that a peak is, in fact, present at ca. 1920 cm^{-1} and that the authors did not assign it due the signal-to-noise ratio.[37] Considering the integrated absorption of the lower frequency peak is only ca. 24% that of the higher frequency peak (see Table 1), we feel this is the most likely explanation. Our results in 10 mol % THF in cyclohexane solution show the formation of both $^3CpCo(CO)$(sol.) and $^1CpCo(CO)$(sol.) from the unsolvated $^3CpCo(CO)$ precursor in the same ratio observed in neat THF solution, and with the same observed frequency for the THF solvated triplet as in the previous study.[6]

Table 1. Relative Spin State Populations[a]

solvent	$^1CpCo(CO)$(sol.) (ca. 1916 cm^{-1})	$^3CpCo(CO)$(sol.) (ca. 1942 cm^{-1})
methanol	29%	71%
1-butanol	21%	79%
1-hexanol	24%	76%
1-decanol	30%	70%
THF	24%	76%

[a]Percentages denote relative integrated peak areas for each absorption.

Voigt lineshapes were fit to the peaks corresponding to the solvated singlet and triplet species in each neat alcohol solvent and neat THF at a time delay of 200 ps. In the case of the absorption at ca. 1942 cm^{-1}, this also required separating a significant overlapping contribution from the parent bleach at ca. 1965 cm^{-1}, to which a Voigt profile was also fit. Undoubtedly, this introduces some amount of error into our values for the peak areas. We also do not have a reliable way of knowing the relative extinction coefficients for the solvated singlet and triplet species. Our main interest here lies in comparing relative populations across different solvents, and since both the singlet and triplet monocarbonyl species have

dx.doi.org/10.1021/ja2098468 | J. Am. Chem.Soc. 2012, 134, 3120−3126

very similar predicted geometries (see DFT calculations), we will make the approximation that the extinction coefficients are equal as we calculate the relative populations of the two species. Table 1 lists the relative peak areas, which, using our assumption of equal extinction coefficients, are equivalent to the relative populations of the solvated singlet and triplet species. The relative populations of the singlet and triplet species are similar in each of these solvents, implying that coordination of CpCo(CO) to the sp^3 oxygen atom in each of these solvents results in similar changes in free energy. The spin state is clearly sensitive to the identity of the moiety directly coordinated to the metal center however, as demonstrated by the results discussed in sections III.A and III.B.

Table 2 summarizes the experimentally observed frequencies for CpCo(CO) photoproducts in each solvent studied.

Table 2. Experimental Frequencies

solvent	solvated photoproduct	observed frequency (cm^{-1})
cyclohexane	^{3}CpCo(CO)	1989
n-octane	^{3}CpCo(CO)	1989
1-chlorobutane	^{1}CpCo(CO)(Cl−R)	1935
1-bromobutane	^{1}CpCo(CO)(Br−R)	1932
1-iodobutane	^{1}CpCo(CO)(I−R)	1932
acetone	^{1}CpCo(CO)(O=CR_2)	1911
DMF	^{1}CpCo(CO)(O=CR_2)	1902
methanol	^{1}CpCo(CO)(HO−R)	1916
	^{3}CpCo(CO)(HO−R)	1942
1-butanol	^{1}CpCo(CO)(HO−R)	1916
	^{3}CpCo(CO)(HO−R)	1942
1-hexanol	^{1}CpCo(CO)(HO−R)	1917
	^{3}CpCo(CO)(HO−R)	1943
1-decanol	^{1}CpCo(CO)(HO−R)	1918
	^{3}CpCo(CO)(HO−R)	1942
THF	^{1}CpCo(CO)(O(−R)$_2$)	1913
	^{3}CpCo(CO)(O(−R)$_2$)	1942

D. Density Functional Theory and ab Initio Calculations. DFT geometry optimizations were carried out to investigate the relative spin state energies of singlet and triplet CpCo(CO) coordinated to each solvent molecule in the study. Each calculation included a single solvent molecule coordinated to the metal center, and thus these are otherwise gas phase calculations of the energies and frequencies for the solvent coordinated species. A careful study of the relative spin state energies for CpCo(CO)[10] has shown that the BP86 functional gives relatively accurate spin state splitting between singlet and triplet states, so we expect the BP86 results to be the most reliable. We checked these calculations against the PW91 functional, which also gave good results in the previous study, and the B3LYP hybrid functional, which gave an excessively large spin state gap in the previous study.[10] Table 3 summarizes the calculated spin state energy differences and frequencies associated with each solvent molecule coordinated to the CpCo(CO) photoproduct in the singlet and triplet states.

Similar to the previous study,[10] we find that the BP86 and PW91 functionals give the best results, while the B3LYP functional consistently overestimates the spin state splitting. We thus focused on the BP86 and PW91 results to draw our conclusions about the observed photoproducts. In the following discussion, results are given as the BP86 value with the PW91 value in parentheses.

Table 3. Results of Density Functional Theory Calculations

	$R_{Co\text{-}X}$ (Å)[a]		frequency (cm^{-1})		
CpCo(CO) +	sing.	trip.	sing.	trip.	ΔE_{T-S}[b] (kcal/mol)
no ligand					
BP86	–	–	1929	1958	−13.0
PW91	–	–	1939	1968	−12.9
B3LYP	–	–	2024	2062	−25.4
1-chlorobutane	X = Chlorine				
BP86	2.25	2.66	1925	1942	7.9
PW91	2.24	2.65	1935	1951	7.7
B3LYP	2.31	2.86	2007	2050	−10.0
1-bromobutane	X = Bromine				
BP86	2.35	2.69	1928	1941	9.4
PW91	2.34	2.68	1937	1949	9.8
B3LYP	2.41	2.91	2008	2046	−8.7
1-iodobutane	X = Iodine				
BP86	2.53	2.83	1928	1944	10.5
PW91	2.52	2.80	1932	1952	11.2
B3LYP	2.58	3.10	2006	2044	−7.8
acetone	X = Oxygen				
BP86	1.88	2.07	1909	1921	11.8
PW91	1.88	2.07	1919	1930	11.9
B3LYP	1.92	2.20	1987	2027	−6.8
DMF	X = Oxygen				
BP86	1.95	2.21	1893	1906	6.6
PW91	1.94	2.20	1903	1916	6.6
B3LYP	1.98	2.22	1975	2029	−8.2
methanol	X = Oxygen				
BP86	2.04	2.24	1914	1927	2.8
PW91	2.03	2.23	1925	1937	2.7
B3LYP	2.03	2.23	2005	2030	−11.5
1-butanol	X = Oxygen				
BP86	2.04	2.29	1919	1927	4.2
PW91	2.04	2.28	1929	1936	4.2
B3LYP	2.04	2.28	2006	2031	−10.2
1-hexanol	X = Oxygen				
BP86	2.04	2.30	1918	1927	4.2
PW91	2.04	2.28	1929	1936	4.3
B3LYP	2.04	2.28	2006	2031	−10.2
1-decanol	X = Oxygen				
BP86	2.04	2.29	1918	1927	4.1
PW91	2.04	2.28	1928	1936	4.1
B3LYP	2.04	2.27	2006	2030	−10.2
THF	X = Oxygen				
BP86	2.02	2.22	1914	1920	4.2
PW91	2.00	2.24	1910	1932	5.8
B3LYP	2.01	2.23	1988	2025	−9.3

[a]Distance between the Co atom and the nearest non-hydrogen ligand atom (X) obtained from optimized geometries. [b]Positive ΔE values indicate the singlet state is favored, while negative values indicate the triplet state is favored.

Looking first at the results in haloalkanes, the predicted energy splitting is 7.9 (7.7) kcal/mol in favor of a solvated singlet photoproduct. The corresponding frequency is predicted to be 1925 (1935) cm^{-1}. While these unscaled frequencies are not expected to match the experimental values exactly, we make use of their relative values with different solvent ligands to assist in making spectral assignments. We have attempted to take a holistic view of the observed and predicted frequencies, calculated energy differences, and

dx.doi.org/10.1021/ja2098468 | J. Am. Chem.Soc. 2012, 134, 3120−3126

experimental data into account in making these assignments. On the basis of the calculated relative spin state energies and comparisons to other observed and predicted frequencies, we assign the experimental peaks at ca. 1935 cm^{-1} in each haloalkane to ^{1}CpCo(CO)(sol.).

In acetone, our calculations predict the solvated singlet species to be favored by 11.8 (11.9) kcal/mol, and the CO stretching frequency is predicted to be 1909 (1919) cm^{-1}. Comparing this calculated frequency to those calculated for the haloalkane solvated complexes, the further red−shifting predicted by coordination to acetone is consistent with the experimentally observed values of ca. 1935 cm^{-1} in haloalkanes and 1911 cm^{-1} in acetone. In DMF, we calculate the solvated singlet to be favored by 6.6 (6.6) kcal/mol, and the predicted frequency is predicted to be even further red-shifted to 1893 (1903) cm^{-1}, again consistent with the experimentally observed frequency of 1902 cm^{-1}.

Moving to the alcohol and THF results, the predicted energy differences for singlet and triplet solvent coordinated species are much smaller. Keeping in mind that these are gas phase calculations, and that entropic contributions are not accounted for, we feel the predicted relative energy differences of ca. 2−4 kcal/mol match the experimental observation of an equilibrium between singlet and triplet spin states reasonably well. We note that none of these functionals include dispersion effects, which could affect the relative stability of singlet and triplet species. Considering the concentration independence and excitation wavelength independence of the observed peak ratios (discussed in section III.B), we were able to independently make the assignment of the two solvated species to ^{1}CpCo(CO)(sol.) and ^{3}CpCo(CO)(sol.), and here we seek primarily to determine which peak corresponds to which spin state. DFT calculations suggest that ^{1}CpCo(CO)(sol.) corresponds to the lower frequency peak, so we tentatively assign solvated singlet CpCo(CO) to the peak at ca. 1916 cm^{-1}, and solvated triplet CpCo(CO) to the peak at ca. 1942 cm^{-1}. By comparison to the spectra and calculations for CpCo(CO) in acetone and DMF, we affirm that the lower frequency absorption at ca. 1916 cm^{-1} corresponds to ^{1}CpCo(CO)(sol.), and thus the absorption at ca. 1942 cm^{-1} corresponds to ^{3}CpCo(CO)(sol.).

As mentioned in section III.B, we feel that the alcohol and THF solvated singlet and triplet species are likely in equilibrium prior to any subsequent reactivity that might occur. One piece of evidence supporting this is the calculated spin-orbit coupling constant of 206.2 cm^{-1} (rms value), which is relatively high among first−row transition metal complexes.[7,38] Recall that the probability of spin state interconversion should scale approximately with the square of this value.[39] The bound singlet and triplet states in alcohols and THF also possess similar geometries, as evidenced by the optimized internuclear distances in Table 3. Looking at the methanol-solvated singlet and triplet structures optimized at the BP86 level, for example, shows an rmsd of only 0.552 Å (0.400 Å with H atoms omitted) in coordinates between the two solvated species.[40] We also performed constrained geometry optimizations at various separations between the oxygen atom of MeOH and the Co metal center for both the singlet and triplet species (Figure 5). This builds approximate potential energy surfaces for the coordination of methanol to singlet and triplet CpCo(CO), which allows us to locate an approximate minimum energy crossing point (MECP) between the two surfaces.[41] The MECP is essentially a transition state analogue for reactions occurring on multiple potential energy surfaces, with the added

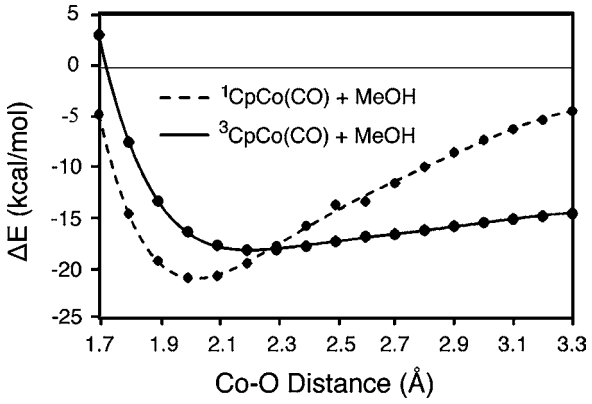

Figure 5. DFT energy scans for coordination of methanol to singlet and triplet CpCo(CO). The curves are generated by performing geometry optimizations at fixed Co−O distances. Circles correspond to calculated energies relative to the dissociation limit on the singlet surface, while the lines are fits to the data presented for visualization purposes only.

constraint that the electronic state must also change in the vicinity of this geometry. We find the MECP to be located at a Co−O separation of 2.28 Å,[42] which is also close to the equilibrium separations of 2.24 and 2.04 Å calculated for the solvated triplet and singlet minima, respectively. The similarity of the MECP to the methanol-solvated minima suggests that crossover between the species is a facile process. Finally, as mentioned above, the experimental spectra show the formation of both photoproducts in their equilibrium ratio from a common unsolvated triplet precursor within the first several picoseconds, strongly suggesting a low barrier to spin state interconversion from the triplet precursor to the solvated singlet species. We feel this is convincing evidence that the two spin states are in equilibrium at ambient temperatures.

IV. CONCLUSIONS

We have shown in this paper that the 16-electron species CpCo(CO) can coordinate to a solvent molecule in either the singlet or triplet spin state. This is in contrast to the previous assertions that triplet 16-electron photoproducts cannot interact strongly with solvent molecules,[7,18,20] and adds to our understanding of triplet reactivity in organometallic photoproducts. The existence of transition metal complexes with two thermally accesible spin states is well known,[43−49] but, to our knowledge, this is the first observation of a transient photoproduct that exhibits an equilibrium between two stable spin states, and also the first observed case in which a solvent molecule has been shown to coordinate to two spin states of the same photoproduct.

In the case of CpCo(CO), spin crossover does not appear to present a significant kinetic barrier to solvent coordination or reactivity of the triplet species, and thus relative thermodynamic stabilities determine the spin state of CpCo(CO) on the picosecond time scale. As electronic structure calculations demonstrate, CpCo(CO) can have favorable interactions with solvent molecules and other ligands in both the singlet and triplet states, and the ability of a solvent ligand to stabilize either state will determine the spin state of the reactant present in solution. These results add to our previous model for triplet reactivity in solution and suggest that the reactivity of triplet photoproducts may depend strongly on how the solvent environment affects the relative spin state energetics. Further

dx.doi.org/10.1021/ja2098468 | J. Am. Chem.Soc. 2012, 134, 3120−3126

experiments are underway to compare the reactivity of solvated singlet and triplet CpCo(CO) as a catalyst in different environments.

■ ASSOCIATED CONTENT

Supporting Information

DFT z-matrix coordinates for all structures listed in Table 3, and complete ref 26. This material is available free of charge via the Internet at http://pubs.acs.org.

■ AUTHOR INFORMATION

Corresponding Author

*cbharris@berkeley.edu

■ ACKNOWLEDGMENTS

This work was supported by NSF's Division of Physical Chemistry. We acknowledge use of the Molecular Graphcis and Computation Facility at UC-Berkeley (grants CHE-0840505, CHE-0233882). This research used resources of the National Energy Research Scientific Computing Center, which is supported by the Office of Science of the U.S. Department of Energy under Contract No. DE-AC02-05CH11231. S.C.N. acknowledges support through a VIED fellowship. J.P.L. acknowledges support through an NSF graduate research fellowship.

■ REFERENCES

(1) (a) Vollhardt, K. P. C. *Acc. Chem. Res.* **1977**, *10*, 1. (b) Vollhardt, K. P. C. *Angew. Chem., Int. Ed. Engl.* **1984**, *23*, 539.

(2) Rest, A. J.; Whitwell, I.; Graham, W. A.; Hoyano, J. K.; McMaster, A. D. *J. Chem. Soc., Dalton Trans.* **1987**, 1181.

(3) Dougherty, T. P.; Heilweil, E. J. *J. Chem. Phys.* **1994**, *100*, 4006.

(4) CrichtonO.RestA. J.TaylorD. J.J. Chem. Soc., Dalton Trans.1980

(5) Bengali, A. A.; Bergman, R. G.; Moore, C. B. *J. Am. Chem. Soc.* **1995**, *117*, 3879.

(6) Wasserman, E. P.; Bergman, R. G.; Moore, C. B. *J. Am. Chem. Soc.* **1988**, *110*, 6076.

(7) Snee, P. T.; Payne, C. K.; Kotz, K. T.; Yang, H.; Harris, C. B. *J. Am. Chem. Soc.* **2001**, *123*, 2255.

(8) Hofmann, P.; Padmanabhan, M. *Organometallics* **1983**, *2*, 1274.

(9) Siegbahn, P. E. *J. Am. Chem. Soc.* **1996**, *118*, 1487.

(10) Carreón-Macedo, J. L.; Harvey, J. N. *J. Am. Chem. Soc.* **2004**, *126*, 5789.

(11) Snee, P. T.; Payne, C. K.; Mebane, S. D.; Kotz, K. T.; Harris, C. B. *J. Am. Chem. Soc.* **2001**, *123*, 6909.

(12) Yang, H.; Kotz, K. T.; Asplund, M. C.; Wilkens, M. J.; Harris, C. B. *Acc. Chem. Res.* **1999**, *32*, 551.

(13) Siegbahn, P. E.; Svensson, M. *J. Am. Chem. Soc.* **1994**, *116*, 10124.

(14) Blomberg, M. R.; Siegbahn, P. E.; Svensson, M. *J. Am. Chem. Soc.* **1992**, *114*, 6095.

(15) Carroll, J. J.; Haug, K. L.; Weisshaar, J. C.; Blomberg, M. R.; Siegbahn, P. E.; Svensson, M. *J. Phys. Chem.* **1995**, *99*, 13955.

(16) Besora, M.; Carreón-Macedo, J. L.; Cowan, A. J.; George, M. W.; Harvey, J. N.; Portuis, P.; Ronayne, K. L.; Sun, X. Z.; Towrie, M. *J. Am. Chem. Soc.* **2009**, *131*, 3583.

(17) Portius, P.; Yang, J.; Sun, X.-Z.; Grills, D. C.; Matousek, P.; Parker, A. W.; Towrie, M.; George, M. W. *J. Am. Chem. Soc.* **2004**, *126*, 10713.

(18) Snee, P. T.; Yang, H.; Kotz, K. T.; Payne, C. K.; Harris, C. B. *J. Phys. Chem. A* **1999**, *103*, 10426.

(19) Kotz, K. T.; Yang, H.; Snee, P. T.; Payne, C. K.; Harris, C. B. *J. Organomet. Chem.* **2000**, *596*, 183.

(20) (a) Yang, H.; Asplund, M. C.; Kotz, K. T.; Wilkens, M. J.; Frei, H.; Harris, C. B. *J. Am. Chem. Soc.* **1998**, *120*, 10154. (b) Yang, H.; Kotz, K. T.; Asplund, M. C.; Harris, C. B. *J. Am. Chem. Soc.* **1997**, *119*, 9564.

(21) (a) Dahy, A. A.; Koga, N. *Bull. Chem. Soc. Jpn.* **2005**, *78*, 781−791. (b) Dahy, A. A.; Suresh, C. H.; Koga, N. *Bull. Chem. Soc. Jpn.* **2005**, *78*, 792−803. (c) Gandon, V.; Agenet, N.; Vollhardt, K. P. C; Malacria, M.; Aubert, C. *J. Am. Chem. Soc.* **2006**, *128*, 8509. (d) Agenet, N.; Gandon, V.; Vollhardt, K. P. C; Malacria, M.; Aubert, C. *J. Am. Chem. Soc.* **2007**, *129*, 8860. (e) Gandon, V.; Agenet, N.; Vollhardt, K. P. C; Malacria, M.; Aubert, C. *J. Am. Chem. Soc.* **2009**, *131*, 3007.

(22) Hamm, P.; Kaindl, R. A.; Stenger, J. *Opt. Lett.* **2000**, *25*, 1798.

(23) (a) Becke, A. D. *J. Chem. Phys.* **1993**, *98*, 5648. (b) Perdew, J. P. *Phys. Rev. B* **1986**, *33*, 8822.

(24) Lee, C.; Yang, W.; Parr, R. G. *Phys. Rev. B* **1988**, *37*, 785.

(25) The PW91 calculations used both PW91 exchange and correlation functionals. (a) Perdew, J. P.; Wang, Y. *Phys. Rev. B* **1992**, *45*, 13244. (b) Perdew, J. P.; Chevary, J. A.; Vosko, S. H.; Jackson, K. A.; Pederson, M. R.; Singh, D. J.; Fiolhais, C. *Phys. Rev. B* **1992**, 6671. (c) Perdew, J. P.; Chevary, J. A.; Vosko, S. H.; Jackson, K. A.; Pederson, M. R.; Singh, D. J.; Fiolhais, C. *Phys. Rev. B* **1993**, 4978.

(26) Frisch, M. J. et al. *Gaussian 09*, Revision B.01; Gaussian: Wallingford, CT, 2009.

(27) (a) Dunning, T. H. *J. Chem. Phys.* **1989**, *90*, 1007. (b) Woon, D. E.; Dunning, T. H. *J. Chem. Phys.* **1993**, *98*, 1358. (c) Balabanov, N. B.; Peterson, K. A. *J. Chem. Phys.* **2005**, *123*, 064107.

(28) Hay, P. J.; Wadt, W. R. *J. Chem. Phys.* **1985**, *82*, 299.

(29) Dunning, T. H.; Hay, P. J. *Methods of Electronic Structure Theory*; Plenum: New York, 1977; Vol. *2*.

(30) Schmidt, M. W.; Baldridge, K. K.; Boatz, J. A.; Elbert, S. T.; Gordon, M. S.; Jensen, J. H.; Koseki, S.; Matsunaga, N.; Nguyen, K. A.; Su, S. J.; Windus, T. L.; Dupuis, M.; Montgomery, J. A. *J. Comput. Chem.* **1993**, *14*, 1347.

(31) Schäfer, A.; Horn, H.; Ahlrichs, R. *J. Chem. Phys.* **1992**, *97*, 2571.

(32) Roos, B. O.; Andersson, K.; Fülscher, M. P.; Malmqvist, P.; Serrano-Andrés L. Pierloot, K. *Adv. Chem. Phys.* **1996**, 219.

(33) Lengsfield, B. H.; Jafri, J. A.; Phillips, D. H.; Bauschlicher, C. W. *J. Chem. Phys.* **1981**, *74*, 6849.

(34) (a) Furlani, T. R.; King, H. F. *J. Chem. Phys.* **1985**, *82*, 5577. (b) King, H. F.; Furlani, T. R. *J. Comput. Chem.* **1988**, *9*, 771. (c) Fedorov, D. G.; Gordon, M. S. *J. Chem. Phys.* **2000**, *112*, 5611.

(35) The parent bands of $CpCo(CO)_2$ recover significantly as the broad bands corresponding to the electronically excited species decay.

(36) O'Connor, J. M.; Casey, C. P. *Chem. Rev.* **1987**, *87*, 307.

(37) Linear interpolation between the data points at 2.2 and 2.3 Å was used to obtain the value of 2.28 Å.

(38) Harvey, J. N.; Aschi, M. *Faraday Discuss.* **2003**, *124*, 129.

(39) Zener, C. *Proc. R. Soc. London A* **1932**, *137*, 696.

(40) Zhurko, G.A.; Zhurko, D.A. *CHEMCRAFT*, Version 1.6 (Build 334).

(41) See for example: Smith, K. M.; Poli, R.; Harvey, J. N. *New J. Chem.* **2000**, *24*, 77.

(42) See Figure 10 of ref 6.

(43) Goodwin, H. A. *Top. Curr. Chem.* **2004**, *234*, 23.

(44) Garcia, Y.; Gütlich, P. *Top. Curr. Chem.* **2004**, *234*, 49.

(45) Goodwin, H. A. *Coord. Chem. Rev.* **1976**, *18*, 293.

(46) Toftlund, H. *Coord. Chem. Rev.* **1989**, *94*, 67.

(47) König, E.; Ritter, G.; Kulshreshtha, S. K. *Chem. Rev.* **1985**, *85*, 219.

(48) Gütlich, P.; Hauser, A.; Spiering, H. *Angew. Chem., Int. Ed. Engl.* **1994**, *33*, 2024.

(49) Gütlich, P.; Garcia, Y.; Goodwin, H. A. *Chem. Soc. Rev.* **2000**, *29*, 419.